Carbohydrate Polymers 83 (2011) 1582–1590

Contents lists available at ScienceDirect

Carbohydrate Polymers

journal homepage: www.elsevier.com/locate/carbpol

# Characterization of biodegradable films from the extracellular polysaccharide produced by *Pseudomonas oleovorans* grown on glycerol byproduct

Vítor D. Alves[a,*], Ana R. Ferreira[b], Nuno Costa[b], Filomena Freitas[b], Maria A.M. Reis[b], Isabel M. Coelhoso[b]

[a] *CEER-Biosystems Engineering, Institute of Agronomy, Technical University of Lisbon, Tapada da Ajuda, 1349-017 Lisbon, Portugal*
[b] *REQUIMTE/CQFB, Chemistry Department, FCT/Universidade Nova de Lisboa, 2829-516 Caparica, Portugal*

ARTICLE INFO

*Article history:*
Received 21 July 2010
Received in revised form 7 September 2010
Accepted 7 October 2010
Available online 13 October 2010

*Keywords:*
Biodegradable films
Microbial polysaccharide
Glycerol by-product
Barrier properties

ABSTRACT

In this work, the film-forming capacity of the new microbial exopolysaccharide (EPS) composed by sugars and acyl groups, produced by *Pseudomonas oleovorans* NRRL B-14682, was studied. The films were transparent and quite flexible and tough when handled, but showed to be stiff under tensile and puncture tests. They presented a high water vapour permeability but a quite low permeability to carbon dioxide, which are typical of hydrophilic polysaccharide films. Furthermore, they showed good stability in contact with liquid water, after auto-crosslinking reactions at low pH, upon or after drying. Preliminary biodegradability tests indicated an easy biological degradation when exposed to soil microorganisms. The results obtained are rather promising regarding the film-forming capacity of the new EPS, as they were obtained only with the biopolymer itself. The films formulation may be complemented with additives (e.g. plasticizers, emulsifiers, nanocomposites), to design films for specific applications.



## 1. Introduction

For a long time traditional polymers have supplied most of common packaging materials because they present several desired features like softness, lightness and transparency. However, increased use of synthetic packaging films has led to serious ecological problems due to their total non-biodegradability (Siracusa, Rocculi, Romani, & Dalla Rosa, 2008). Consequently, the interest on replacing conventional polymers in some packaging applications by biopolymers, has greatly increased, as they are biodegradable and can be produced or recovered from renewable resources.

Water soluble polysaccharides, such as starch, pectin, alginate, carrageenan, chitosan and cellulose derivates, are known for their film-forming properties which have been intensively investigated (Aider, 2010; Alves, Costa, & Coelhoso, 2010; Bertuzzi, Vidaurre, Armada, & Gottifredi, 2007; da Silva, Bierhalz, & Kieckbusch, 2009; de Moura et al., 2009; Fabra, Talens, & Chiralt, 2008; Lafargue, Lourdin, & Doublier, 2007). Due to the large diversity of available polysaccharides, a wide range of films properties can be obtained (Nisperos-Carriedo, 1994).

The referred polymers are commonly extracted from natural resources, such as plants and algae, as well as from agro-industrial by-products. However, the recovery process is generally based on the use of chemicals (Hilliou et al., 2006). Furthermore, the availability and quality of the biopolymer sources are dependent on climate and on the season of the year. As a consequence, the properties of the polymer recovered present a significant variability over time.

Microbial polysaccharides represent an alternative to those obtained by other processes. Hyaluronan, kefiran and gellan are examples of microbial polysacharides that have been tested to produce biodegradable films (Piermaria, Pinotti, García, & Abraham, 2009; Sun & Zhitomirsky, 2009; Xu, Li, Kennedy, Xie, & Huang, 2007). Xanthan gum has also been used in blends with other biopolymers (Soares, Lima, Oliveira, Pires, & Soldi, 2005). In microbial processes, after process optimization, the cultivation parameters (e.g. stirring rate, temperature, pH, nutrients concentration) are easily controlled over time, enabling the production of biopolymers with rather stable chemical and physical characteristics. Nevertheless, the potential market of these biopolymers is still conditioned by the production costs, which are quite dependent on the high price of the carbon sources commonly used, such as sucrose and glucose (García-Ochoa, Santos, Casas, & Gómez, 2000; Singh, Saini, & Kennedy, 2008). As such, the attention has been driven to search viable low-cost carbon sources, namely among agro-industrial wastes and industrial by-products. Glycerol rich by-product from the biodiesel production is an example. It is generated in large quantities, far beyond current consumption in traditional applications, and the development of new routes to convert crude glycerol into higher value products is an urgent need.

* Corresponding author. Tel.: +351 213653546; fax: +351 213653195.
*E-mail address:* vitoralves@isa.utl.pt (V.D. Alves).

0144-8617/$ – see front matter © 2010 Elsevier Ltd. All rights reserved.
doi:10.1016/j.carbpol.2010.10.010

It was stated that the glycerol present on the glycerol-rich by-product from biodiesel production can be applied as carbon source to produce a new extracellular polysaccharide (EPS) using a *Pseudomonas* strain, with attractive productivities and polymer yield. The new EPS is a high molecular weight negatively charged heteropolysaccharide, composed by sugars (galactose, glucose, mannose and rhamnose) and acyl groups (pyruvil, succynil and acetyl have been identified) (Freitas, Alves, Carvalheira, et al., 2009).

In this work, the ability of the new EPS to produce biodegradable films was studied. The films were characterized in terms of their hygroscopic, mechanical and barrier properties. Their stability in contact with liquid water was evaluated, by the measurement of solubility in water and swelling degree. Preliminary biodegradability studies were performed, in order to perceive the films biological degradation rate when exposed to soil microorganisms. Anticipating applications in which a good transparency is required (e.g. food packaging), the colour alterations due to film application were also studied.

## 2. Materials and methods

### 2.1. Exopolysaccharide production and characterization

The biopolymer was produced by *Pseudomonas oleovorans* NRRL B-14682 grown on a slightly modified Medium E* supplemented with glycerol byproduct, in a 10-L bioreactor (Biostat B-plus, Sartorius) (Freitas, Alves, Pais, et al., 2009). The cultivation included an initial batch phase (~24 h), followed by a fed-batch phase, wherein the bioreactor was fed with cultivation Medium E*, containing 200 g $L^{-1}$ of glycerol at a constant rate (20 mL $h^{-1}$) (Freitas, Alves, Carvalheira, et al., 2009).

Polymer extraction was performed as described by Freitas, Alves, Carvalheira, et al. (2009). Briefly, the cultivation broth was diluted with deionised water for viscosity reduction, centrifuged for cell separation and precipitated by the addition of cold acetone (3:1). The precipitated polymer was washed with acetone, dissolved in deionised water, freeze-dried and stored.

The exopolysaccharide was analyzed in terms of its sugar and acyl groups composition, as well as its inorganic and protein content. The constituent monosaccharides and acyl groups were quantified in the acid hydrolysate of the polymer, as described by Freitas, Alves, Carvalheira, et al. (2009). Total protein content was determined based on the Lowry method, as described by Freitas, Alves, Carvalheira, et al. (2009). The total inorganic content of the biopolymer was evaluated by subjecting it to pyrolysis at a temperature of 550 °C for 48 h (Hilliou et al., 2009). Average molecular weights ($M_w$) and the polydispersity index ($M_n/M_w$) were obtained by size exclusion chromatography, as described by Freitas, Alves, Pais, et al. (2009).

### 2.2. Films preparation

#### 2.2.1. Filmogenic solutions

The solutions were prepared starting directly from the cultivation broth. A broth volume of 250 ml was diluted with deionised water (1:3) and the biomass separated by centrifugation. A 100% (w/v) trichloroacetic acid (TCA) solution was added to the supernatant (1:10), and a second centrifugation step was used to separate the precipitated proteins and residual cell debris. The polysaccharide was then precipitated from the treated supernatant by the addition of acetone (1:3), recovered, and dissolved immediately in deionised water (120 ml), in order to obtain a polymer concentration of about 0.49% (dry weight). Sodium azide (10 ppm) was added to prevent microbial growth.

#### 2.2.2. Rheology of filmogenic solutions

The viscosity and viscoelastic properties of the polysaccharide solutions were studied using a controlled stress rheometer (Haake RS-75, Germany), equipped with a cone and plate geometry (diameter 3.5 cm, angle 2°). Flow curves were determined using a steady state flow ramp in the range of shear rate from 2.4 to 520 $s^{-1}$. Experimental results were fitted to Eq. (1) with the purpose of estimating the zero shear rate viscosity, which is, in fact, the viscosity of the solution in the beginning of the drying process.

$$\eta_a = \frac{\eta_0}{1 + (\tau\dot{\gamma})^m} \quad (1)$$

where $\dot{\gamma}$ is the shear rate ($s^{-1}$), $\eta_a$ is the apparent viscosity (Pa s), $\eta_0$ is the zero-shear rate viscosity (Pa s), $\tau$ is a time constant (s) and $m$ is a dimensionless constant. Eq. (1) is obtained from the Cross equation assuming a negligible viscosity of the second Newtonian plateau when compared to $\eta_a$ and $\eta_0$, which is valid in this work since the second Newtonian plateau was never approached. Frequency sweeps were carried out at controlled stress (1.5 Pa), within the linear viscoelastic region, to measure the dynamic moduli $G'$ and $G''$, before and after the steady state tests. The sample area exposed to air was covered with paraffin oil in order to prevent water loss. Two replicates were performed for each test.

#### 2.2.3. Production of films

After removing the air bubbles under vacuum, the solutions were transferred to Teflon Petri dishes and dried at 30 °C to form a film. Films thickness was measured in at least six points with a manual micrometer (Braive Instruments). The films were stored at a specific relative humidity and temperature, depending on the tests to be performed.

### 2.3. Colour measurements

The colour alterations on objects due to the application of the films prepared was evaluated by measuring the colour parameters of coloured paper sheets, covered and uncovered by the test films. A Minolta CR-300, USA, colorimeter was used, and the CIELAB colour space was applied with the calculation of colour differences ($\Delta E_{ab}$), chroma ($C_{ab}$) and hue ($h_{ab}$), according to the following equations:

$$\Delta E_{ab} = [(\Delta L^*)^2 + (\Delta a^*)^2 + (\Delta b^*)^2]^{1/2} \quad (2)$$

$$C_{ab} = [a^{*2} + b^{*2}]^{1/2} \quad (3)$$

$$h_{ab} = \arctan\left(\frac{b^*}{a^*}\right) \quad (4)$$

Ten measurements on different areas of the coloured paper sheets, with and without films, were performed.

### 2.4. Water sorption isotherms

Water sorption isotherms were determined by a gravimetric method at 30 °C. Samples with dimensions of 30 mm × 30 mm were previously dried at 70 °C during 24 h. The samples were then placed in desiccators with different saturated salt solutions: LiCl, $CH_3COOK$, $K_2CO_3$, $NaNO_2$, KBr, $BaCl_2$ and $K_2SO_4$, with a water activity at 30 °C of 0.113, 0.220, 0.437, 0.648, 0.803, 0.920 and 0.970, respectively (Greenspan, 1977; Labuza, Kaanane, & Chen, 1985). The samples were weighed after 3 weeks, ensuring that the equilibrium has been reached. Three replicates were performed for each water activity value. The Guggenheim-Anderson-de Boer (GAB) model (Eq. (5)) was used to fit the experimental sorption data.

$$X = \frac{CkX_0a_w}{[(1 - ka_w)(1 - ka_w + Cka_w)]} \quad (5)$$

where $X$ is the equilibrium moisture content at the water activity $a_w$, $X_0$ is the monolayer moisture content, $C$ is the Guggenheim constant and represents the energy difference between the water molecules attached to primary sorption sites and those absorbed to successive sorption layers, and $k$ is the corrective constant taking into account properties of multilayer molecules with respect to the bulk liquid. GAB equation parameters were calculated by non-linear fitting using the software package Scientist™, from MicroMath®.

### 2.5. Swelling degree and solubility in water

After determining the weight ($W_i$) and the volume ($V_i$) of dried film samples (30 mm × 30 mm), they were immersed in deionised water for 24 h, after which their volume ($V_f$) and weight ($W_f$) were measured again. The swelling degree was determined in terms of weight and volume, according to Eqs (6) and (7), respectively:

$$\text{Swelling}_w \ (\%) = \frac{W_f - W_i}{W_i} \times 100 \quad (6)$$

$$\text{Swelling}_{vol} \ (\%) = \frac{V_f - V_i}{V_i} \times 100 \quad (7)$$

The weight after immersion was measured after removing carefully the excess water on the films surface using a paper tissue; while the initial volume and the volume after immersion were calculated by measuring the dimensions of the films with a micrometer and a Vernier caliper.

The samples were dried again, and the solubility was calculated based on the decrease of their dry weight (Eq. (8)):

$$\text{Solubility} \ (\%) = \frac{(\text{initial dry weight} - \text{final dry weight})}{(\text{initial dry weight})} \times 100 \quad (8)$$

The procedure was repeated three times.

### 2.6. FTIR measurements

The infrared spectra of the exopolysaccharide sample films and commercial sodium alginate, were acquired with a Nicolet Nexus spectrophotometer interfaced with a Continuum microscope, using a MCT-A detector cooled by liquid nitrogen. All the spectra presented were obtained in transmission mode, using a *Thermo* diamond anvil compression cell. The spectra were obtained, in a 100 μm × 100 μm area, with a resolution 8 $cm^{-1}$ and 128 scans. The $CO_2$ absorption band at approximately 2300–2400 $cm^{-1}$ was removed.

### 2.7. Mechanical properties

Tensile and puncture tests were carried out using a TA-Xtplus texture analyser (Stable Micro Systems, Surrey, England). In the first case, film strips (20 mm × 70 mm) were attached on tensile grips A/TG and stretched at 0.5 mm/s in tension mode. The tensile stress at break was calculated as the ratio of the maximum force to the films cross-sectional area. The elongation at break was determined as the ratio of the extension of the sample upon rupture by the initial gage length. Puncture tests were carried out immobilizing the test film (30 mm × 30 mm) on a specially designed base with a hole of 10 mm in diameter. The samples were compressed at a speed of 1.0 mm/s and punctured through the hole with a cylindrical probe (2 mm diameter). The puncture stress was expressed as the ratio of the puncture strength by the probe contact area. All mechanical tests were performed at 22.0 ± 2.0 °C, and the samples were equilibrated at 44.3% relative humidity and 19.0 ± 2.0 °C. Five replicates of each film were analyzed.

### 2.8. Water vapour permeability

The water vapour permeability was measured gravimetrically at 30 °C. The films samples were sealed with silicone to the top of a glass Petri dish with a diameter of 5 cm and placed in a desiccator containing a saturated salt solution and equipped with a fan to promote air circulation. Room temperature and relative humidity inside the desiccator were monitored over time using a thermohygrometer (Vaisala, Finland). Two different driving forces were imposed. In the first one, a saturated $NaNO_2$ solution was used inside the Petri dish (RH = 64.8%), placed in a desiccator containing a saturated $CH_3COOK$ solution (RH = 22.0%). The water vapour permeability was measured using films conditioned previously at a relative humidity of 64.8%. The second driving force tested was imposed using a saturated $BaCl_2$ solution (RH = 92.0%) inside the Petri dish and a saturated $NaNO_2$ solution outside (RH = 64.8%), and the films tested were previously equilibrated at a relative humidity of 92.0%. The water vapour flux was determined by weighing the Petri dish in regular time intervals for 8 h. Three independent runs were performed for each driving force.

The water vapour permeability (WVP) was calculated using Eq. (9).

$$WVP = \frac{N_w \times \delta}{\Delta P_{w,eff}} \quad (9)$$

In which, $N_w$ is the water vapour molar flux, $\delta$ is the film thickness and $\Delta P_{w,eff}$ is the effective driving force, expressed as the water vapour pressure difference between both sides of the film, calculated taking into account the mass transfer resistance of the stagnant film of air below the test film, based on the method described by Gennadios, Weller, and Gooding (1994).

The permeability may be expressed as the product of the water sorption coefficient ($S$) to the effective water diffusion coefficient ($D_{eff}$). Their relative contribution to the overall permeability is dependent on the films internal structure and on the affinity of the diffusing molecules towards the film material. The effective water diffusion coefficient was calculated using the methodology described by Alves et al. (2010), which expresses the molar water flux ($N_w$) through the test film at steady-state using an equation based on the first Fick's law:

$$N_W = \frac{D_{eff}\rho_s}{M_w}\frac{X_1 - X_2}{\delta} \quad (10)$$

In which $\rho_s$ is the dry film density, $M_w$ is the water molar mass, $X_i$ is the water concentration (dry basis) in both film interfaces ($X_1 > X_2$) and $\delta$ is the film thickness. At equilibrium, $X_i$ values may be related to the water activity using the water sorption isotherms by Eq. (11) (Larotonda, Matsui, Sobral, & Laurindo, 2005):

$$S_i^* = \frac{X_i}{a_{wi}} = \tan(\theta) \quad (11)$$

where $S_i^*$ [$g_{water}/g_{solids}$] is the water sorption coefficient of the film material, which was calculated graphically. In order to define the sorption coefficient in terms of $g_{water}/g_{solids}$ Pa, $S_i^*$ was divided by the water vapor saturation pressure at the isotherm temperature ($P_w^*$):

$$S_i = \frac{X_i}{a_{wi}P_w^*} \quad (12)$$

Combining Eqs. (10) and (12), an expression which enables the determination of the effective diffusion coefficient, is obtained:

$$D_{eff} = \frac{N_W M_w}{\rho_s P_w^*(S_1 a_{w1} - S_2 a_{w2})} \quad (13)$$

### 2.9. Gas permeability

The experimental apparatus used is composed of a stainless steel cell with two identical chambers separated by the test film supported on a macroporous stainless steel support. The films were equilibrated at 30 °C in a desiccator containing a saturated $K_2CO_3$ solution, with a water activity of 0.437, and presented a water content of 7 ± 2% (dry basis) in the beginning of each experiment. Film thickness was measured after water vapour adsorption equilibrium. The permeability was evaluated by pressurizing one of the chambers (feed) up to 0.7 bar, with pure carbon dioxide, followed by the measurement of the pressure change in both chambers over time, using two pressure transducers (Druck, PDCR 910 model). High-purity grade carbon dioxide (99.998%) Praxair, Spain, was used. Three independent measurements were made at constant temperature, 30 °C, using a thermostatic bath (Julabo, Model EH, Germany). The permeability was calculated as described by Alves et al. (2010).

### 2.10. Biological degradation

The biodegradability test was carried out using a mixed microbial culture obtained from a soil sample. A nutrient medium, composed by tryptone (5 g), yeast extract (2.5 g) and NaCl (5 g) in 500 ml of water, was mixed with 100 g of soil. The suspension was decanted and filtered, and the filtrate was incubated at 30 °C for 24 h, to obtain a grown and viable inocullum. EPS film samples (3 cm × 3 cm) were placed in Petri dishes with the culture medium supported in nutrient agar and inoculated with the microbial culture prepared. The Petri dishes were placed in a desicator with a relative humidity of 90%, at 30 °C, in the dark, for 28 days. Along with the EPS films, samples of a biodegradable film (κ-carrageenan) and of a non-biodegradable polymer LDPE, low density polyethylene were also tested, as positive and negative case studies, respectively.

## 3. Results and discussion

### 3.1. Exopolysaccharide production and chemical characterization

The conditions for production of the biopolymer used in this study were described previously (Freitas, Alves, Carvalheira, et al., 2009). *P. oleovorans* was grown on glycerol byproduct as the sole carbon source, under controlled temperature and pH (30 ± 0.1 °C and 6.8 ± 0.05, respectively), and constant air flow rate (1 vvm, volume of air per volume of reactor per minute). At the end of the batch phase (1 day), bacterial cell growth was suppressed by imposing nitrogen limiting conditions (<0.1 g $NH_4^+$ $L^{-1}$) in the bioreactor. Under these conditions, EPS synthesis was initiated and reached a concentration of 15.0 g $L^{-1}$ within 5 days of cultivation. Considering the time window of effective EPS production (between days 1 and 5), there was a productivity of 0.13 g $L^{-1}$ $h^{-1}$. This productivity is in the range of values reported for xanthan gum (0.13–0.51 g $L^{-1}$ $h^{-1}$) (García-Ochoa et al., 2000) produced under optimized conditions using glucose and/or sucrose as carbon sources.

The glycosyl composition analysis revealed that galactose was the most abundant monosaccharide constituent of the EPS, representing 68% of the polymer's carbohydrate content. Mannose, glucose and rhamnose were also present, accounting for 17, 13 and 2%, respectively. The polymer also had acyl groups substituents, namely, pyruvil and succinyl, which accounted for 2.51 and 0.54%, respectively, of the dry polymer's mass. The extracted polymer also contained some remnants of the culture broth, namely, proteins and inorganic residues that co-precipitated along with the EPS by the addition of acetone. Proteins accounted for 10% of the polymer's mass, while the total inorganic residues content was 8.2%. After a purification step, consisting on the addition of TCA to an aqueous freeze-dried EPS solution followed by centrifugation to separate the precipitate formed, both proteins and inorganic residues were completely removed. The average molecular weight of the EPS was $4.6 \times 10^6$ with a polidispersity index of 2.33, which indicates the polymer is rather homogeneous.

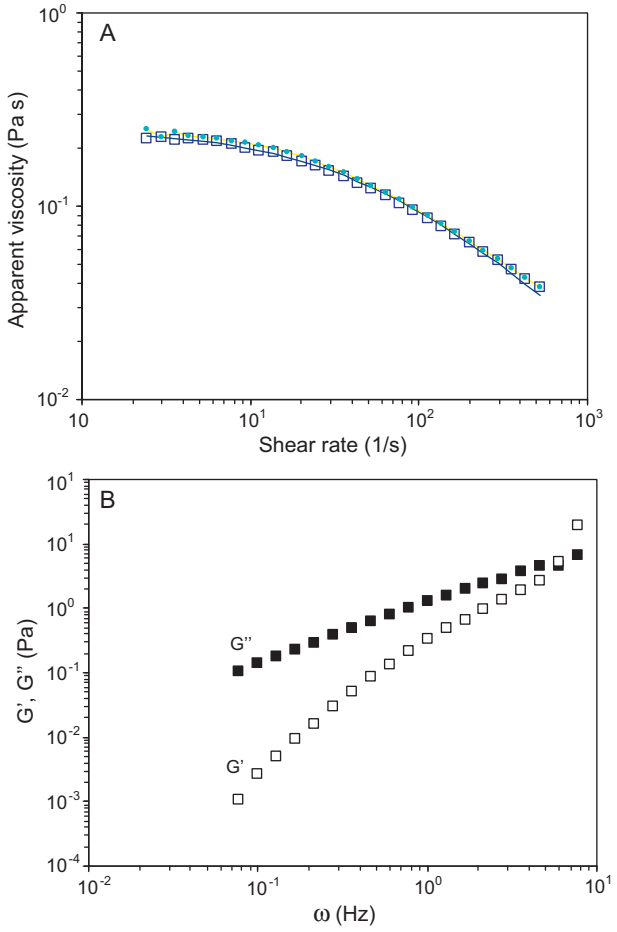


**Fig. 1.** (A) Flow curve of the film-forming solution: (□) experimental data for shear rate from 2.4 to 520 $s^{-1}$, (●) experimental data for shear rate from 520 to 2.4 $s^{-1}$; (—) fitting to Eq. (8). (B) Mechanical spectrum of the film-forming solution.

### 3.2. Rheology of filmogenic solutions

The flow curve of the EPS solution prepared directly from the cultivation broth, with an intermediate treatment with TCA, is presented in Fig. 1A. The solution presents a non-Newtonian shear thinning behaviour, showing the first Newtonian plateau at low shear rates. Eq. (1) fitted quite well the experimental results (Fig. 1A), with the following parameter values: $\eta_0 = 0.252 \pm 0.003$ Pa s; $\tau = 0.0196 \pm 0.001$ s and $m = 0.792 \pm 0.020$ ($r^2 = 0.999$). It was also observed that the apparent viscosity is immediately recovered when the shear rate was decreased, after exposing the sample to shear rates as high as 520 $s^{-1}$ (Fig. 1A). The same behaviour was already perceived for EPS solutions from the freeze-dried polymer, without TCA treatment (Freitas, Alves, Carvalheira, et al., 2009).

Regarding the viscoelastic properties, the mechanical spectrum obtained (Fig. 1B) shows a viscous modulus ($G''$) higher than the elastic modulus ($G'$), with a crossover at high frequencies. This is the behaviour of a viscous solution with entangled polymer chains. The mechanical spectra measured before and after the steady shear

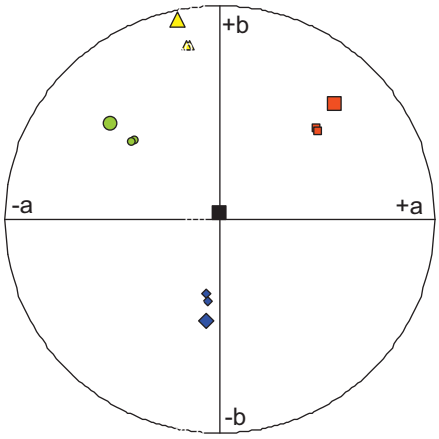


| Colour | $\Delta E_{ab}$ |
|---|---|
| Red | 11.3±0.4 |
| Yellow | 9.9±0.4 |
| Green | 9.6±0.3 |
| Blue | 6.9±1.8 |
| Black | 10.2±0.2 |

**Fig. 2.** Parameters $a^*$ and $b^*$ of the CIELAB system for coloured paper sheets uncovered (large symbols) and covered (small symbols) by the test films. In the insert is presented the colour differences calculated using Eq. (2).

tests were coincident, confirming the inexistence of strong interactions which could be broken down.

### 3.3. Films appearance and colour alteration

The films prepared were quite transparent, flexible and tough when handled, and could be easily bended without breaking. Colour changes of objects due to the application of the films were evaluated by measuring the colour parameters of coloured paper sheets, uncovered and covered by two sample films. Fig. 2 presents the CIELAB colour parameters $a^*$ and $b^*$, for each colour tested. It may be observed that, for all cases, the hue ($h_{ab}$, angle towards the horizontal axes) does not change with the application of the film. However, colour saturation ($C_{ab}$) presents a small decrease, the dots move towards the origin, meaning that the colour becomes less vivid. The colour alterations due to film application are quite low, $\Delta E_{ab} \leq 11.3$ (see insert in Fig. 2), indicating a film with a rather good transparency. Nevertheless, the colour differences may be significant enough to be perceived by the human eye.

### 3.4. Water sorption isotherms

The water sorption isotherm of the films obtained is presented in Fig. 3, along with data for pectin and κ-carrageenan films, determined in a previous work (Alves et al., personal communication), for comparison. It can be observed that the EPS films are quite hygroscopic. The water vapour sorption capacity increases slowly for water activity values below 0.648, after which there is a sudden increase. The affinity towards water vapour is similar to that of pectin, but lower when compared to κ-carrageenan, for $a_w < 0.92$. The GAB model fitted well the experimental results ($X_0 = 0.047 \pm 0.009$, $k = 0.959 \pm 0.010$ and $C = 2.08 \pm 2.59$; $r^2 = 0.99$).

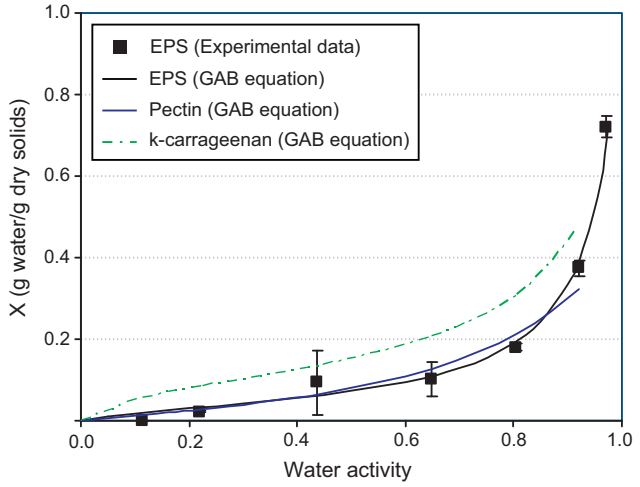


**Fig. 3.** Water sorption isotherms of EPS films at 30 °C (symbols), and GAB equation for EPS, pectin and κ-carrageenan films (lines).

### 3.5. Swelling degree and film solubility in water

Film samples (30 mm × 30 mm) were immersed in deionised water for 24 h. The films obtained directly from the cultivation broth, with TCA treatment, have maintained completely their physical integrity. Furthermore, they presented a high swelling degree, both in weight (102.7 ± 9.1%) and in volume (70.0 ± 16.5%). Their water solubility was rather low, as only about 4% of the initial mass of dry film was dissolved. This behaviour was somewhat unexpected, since the films were produced from filmogenic solutions, consisting on EPS dissolved in water. Moreover, it was also observed that films produced from aqueous solutions of freeze-dried polymer, obtained without any TCA treatment, have dissolved easily. The main difference between the two preparation methods was the application of the purification step with TCA. Acid addition lowered the pH of the filmogenic solution, which may have promoted the formation of strong interactions between polymer chains, making the films resistant to liquid water. There are references in the literature of such strong interactions between polysaccharide chains in acidic media. Okamoto and Miyoshi (2002) and Collins and Birkinshaw (2008) have performed auto-crosslinking of hyaluronic acid under acidic conditions, which may be due to esterification reactions between carboxyl and alcohol groups present in the same or in different polymer chains. This process may well be occurring with the EPS films when TCA is added.

Crosslinking reactions would create a structured polymer network in the filmogenic solution that should be reflected on its mechanical spectrum (Fig. 1B), with a storage modulus higher than the loss modulus and both less dependent on the frequency variation, which was not the case. It seems that those reactions are not occurring extensively on the filmogenic solution before drying. In fact, Okamoto and Miyoshi (2002) have produced hyaluronic acid (HA) hydrogels with auto-crosslinking reactions at low pH, but using a freezing process. Those authors claim that the electrostatic repulsive forces between the HA molecules are suppressed so the HA molecules are packed closely together to facilitate the formation of a gel. A similar mechanism might be occurring with EPS films. Crosslinking reactions are probably taking place extensively only during drying process, in which the polymer molecules are driven to a closer contact and packed, as water evaporates.

### 3.6. FTIR analysis

FTIR analysis of dried film samples was performed in order to evaluate the occurrence of such auto-crosslinking reactions. Fig. 4 shows the spectra obtained for a water soluble film prepared from an aqueous solution of the freeze-dried polymer, without any TCA treatment, (Fig. 4(d)) and for a film sample obtained from the cultivation broth with the intermediate TCA treatment (Fig. 4(c)). An additional film was prepared by immersion of a water soluble film sample in an acetone:water mixture (80:20) with hydrochloric acid at pH 2. The film thus obtained became insoluble in water (Fig. 4(b)). It is also presented the spectrum of sodium alginate, a negatively charged hydrophilic polyelectrolyte (Fig. 4(a)).

It can be seen, for all cases, a broad and intense band around 3400 $cm^{-1}$, representing O–H stretching of hydroxyls and bound water (Synytsya, Copikova, Matejka, & Machovic, 2003), over-

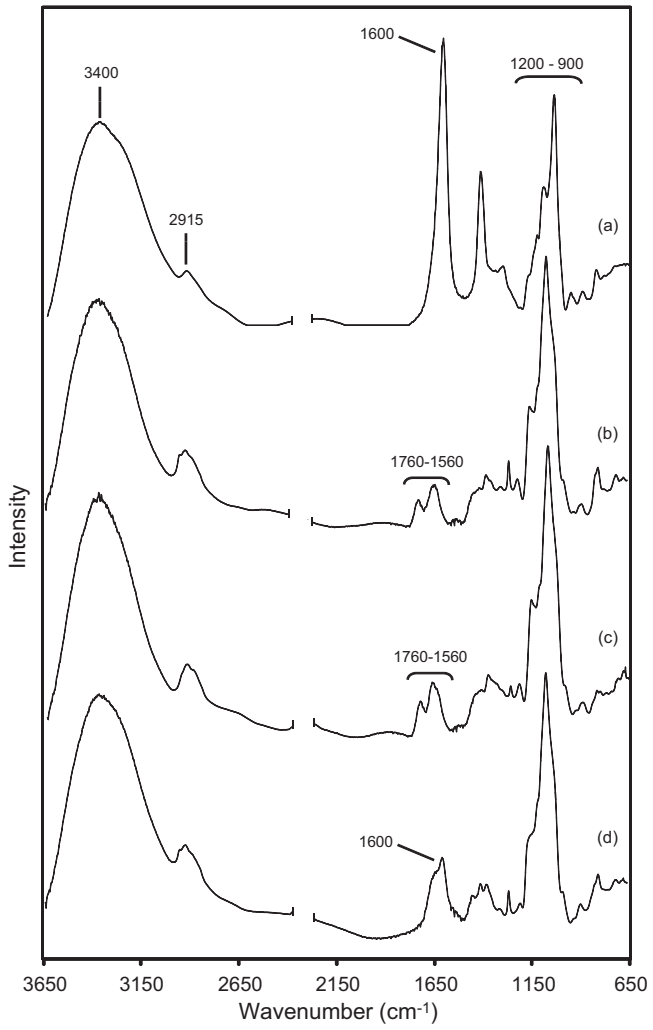


**Fig. 4.** FTIR spectra: (a) sodium alginate, (b) EPS film after immersion in a acetone–water mixture at pH 2, (c) EPS film prepared with the intermediate treatment with TCA, (d) EPS film soluble in water, prepared from the freeze-dried polymer.

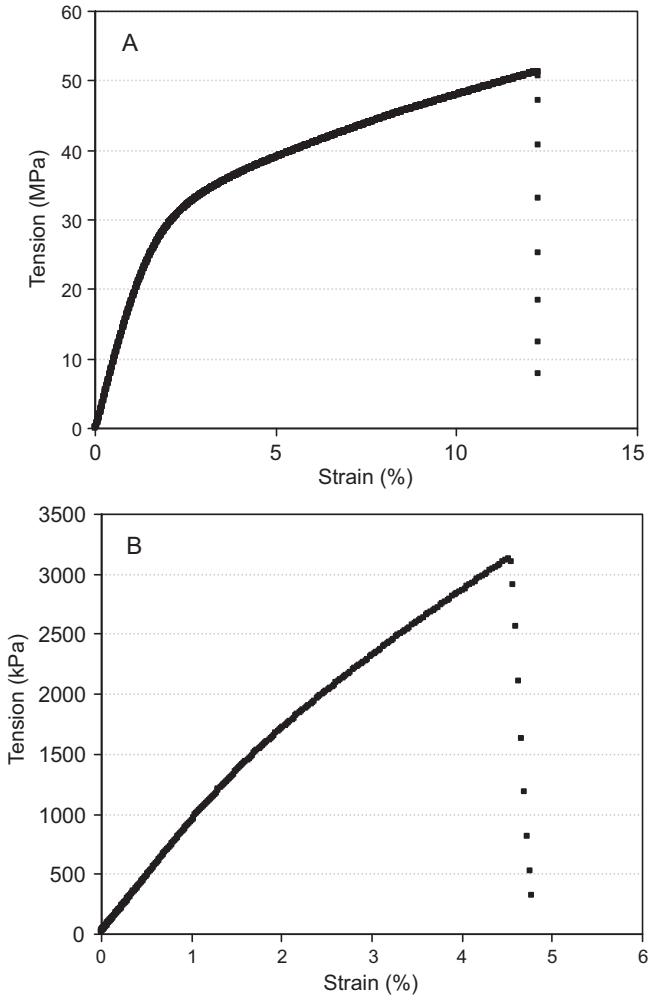


**Fig. 5.** Representative stress–strain curves of the films prepared with the intermediate TCA treatment: (A) tensile tests, (B) puncture tests.

lapping the C–H stretching peak of $CH_2$ groups appearing at 2915 $cm^{-1}$. The region around 1200–900 $cm^{-1}$, also common to all samples, represents skeletal C–O and C–C vibration bands of glycosidic bonds and pyranoid ring (Synytsya et al., 2003). The strong band around 1600 $cm^{-1}$ in alginate spectrum, which can be attributed to the asymmetric stretching of carboxylates (Synytsya et al., 2003), is also observed in the water soluble film spectrum, but not in the same way in the spectrum of the samples that were in contact with an acidic medium. In fact, for those samples, two bands appear in a region, from 1760 to 1560 $cm^{-1}$, attributed to stretching of C=O bonds, not only on carboxylic groups, but also in ester groups. This fact indicates the formation of ester linkages, involving the carboxylic and hydroxyl groups of the polymer chains (auto-crosslinking), when the dried polymer (or upon drying) is contacted with a medium at low pH.

### 3.7. Mechanical properties

The crosslinked film samples were subjected to tensile tests, after being equilibrated at RH = 44.3% and 19 ± 2 °C, presenting 10 ± 2% of water (dry weight). A typical stress–strain curve is presented in Fig. 5A, and the calculated parameters are shown in Table 1, along with the values referred in the literature for films from biopolymers extracted from vegetal and animal sources, and synthetic polymers (PP and HDPE). Even though the EPS films could be easily bended without breaking, they have shown to be stiff when subjected to tensile tests, revealing a low strain at break (9.5 ± 3.9%), a high Young modulus (1738 ± 114 MPa) and a stress at break of 51 ± 3 MPa. These values are in the same order of magnitude as those referred for chitosan, corn starch and κ-carrageenan, with similar water content. Cassava starch films behave very differently, with a much higher strain at break and a lower Young modulus, which are, even so, very far from the good mechanical properties of PP and HDPE. The stiffness of the EPS films was also evident on the puncture tests (typical curve presented in Fig. 5B), in which they presented a rather low deformation at break (3.8 ± 0.6%) and a high tension at break (2959 ± 261 kPa). It should be emphasized that the EPS films were prepared with no addition of plasticizers or other additives, as well as the polysaccharide films referred in Table 1. As so, stiff films from these materials were expected. Furthermore, the auto-crosslinking reaction in acidic media with the creation of a polymer network, is probably also contributing for the high EPS films stiffness.

The results obtained are rather promising regarding the ability of the novel microbial polysaccharide to produce films, as they were obtained only with the biopolymer itself. The aqueous formulation may be further designed to form films for specific applications, with the incorporation of additives (e.g. plasticizers, emulsifiers, nanocomposites), or blending with other compatible biopolymers.

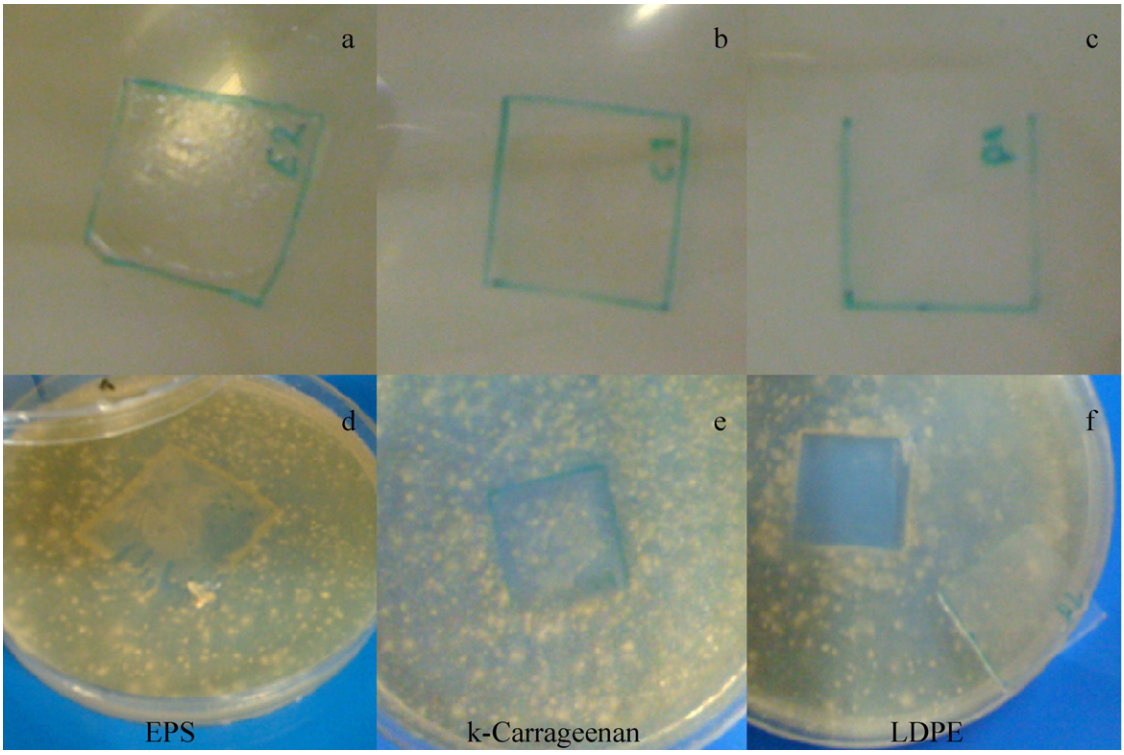


**Fig. 6.** Photos of EPS, κ-carrageenan and LDPE film samples at the beginning (a, b, c) and at the end (d, e, f) of the biological degradation test.

### 3.8. Water vapour permeability and diffusion coefficients

The obtained values for effective water vapour driving force ($\Delta P_{w,eff}$), calculated taking into account the mass transfer resistance of the stagnant film of air below the test film, were $494 \pm 25$ and $1451 \pm 100$ Pa, for the experiments using the relative humidity differences 92.0–64.8% and 64.8–22.0%, respectively, at $T = 30 \pm 0.5$ °C. Table 2 summarizes the estimated values for the diffusion coefficients, using Eq. (13), along with the calculated sorption coefficients (Eqs. (11) and (12)), and the measured water vapour permeability (WVP).

The water vapour permeability was about five times higher when the ΔRH (%) of 92.0–64.8 was applied. This fact is due to the much higher water vapour sorption coefficients at a RH of 92%, when compared to the water vapour sorption capacity of the film at RH = 64.8% and RH = 22.0%. For the conditions studied, the WVP is fully controlled by the water vapour solubility ($S$), since the estimated effective water diffusion coefficients were quite similar for both driving forces tested.

Water diffusivity depends on the interactions between water molecules and the polymeric matrix. The water adsorbed acts as a plasticizer and loosens the matrix facilitating water diffusion. As a consequence, it could be expected an increase of water diffusivity as the amount of adsorbed water increased. The increase of the films thickness was measured after gas–solid equilibrium of dried samples subjected to RH = 22.0%, 64.8% and 92.0% at 30 °C. The results have shown a slight thickness increase, from $3.7 \pm 1.6$% at RH = 22.0% up to $10.4 \pm 1.7$% at RH = 92.0%, from which it may be concluded that the films thickness and swelling do not change significantly with relative humidity. The crosslinked polymer matrix may be limiting films swelling when they are in contact with water vapour. The looseness of the matrix does not increase significantly when the films are exposed to higher RH values, even though the amount of water adsorbed is higher, due to the bonds between polymer chains that constrain films swelling. As a consequence, no significant changes are observed on the diffusivity.

The WVP values obtained are in the same order of magnitude of those determined for pectin/κ-carrageenan films

**Table 1**
Mechanical properties of EPS films, along with those of other polymers referred in the literature.

| Film | % Water (dry basis) | Stress at break (MPa) | Elongation at break (%) | Young modulus (MPa) | Reference |
|---|---|---|---|---|---|
| EPS | 10 | $51 \pm 3$ | $9.5 \pm 3.9$ | $17385 \pm 114$ | Present study |
| Chitosan | 15 | 100 | 16.0 | 1481 | Lazaridou and Biliaderis (2002) |
| Corn starch | 12 | 48 | 2.0 | 1229 | Mali, Grossmann, García, Martino, and Zaritzky (2006) |
| κ-Carrageenan | 19 | 57 | 6.8 | 1110 | Lafargue et al. (2007) |
| Cassava starch | 12 | 1.3 | 66.7 | 21.7 | Müller, Laurindo, and Yamashita (2009) |
| Sodium alginate[a] | 24 | 72 | 3.5 | – | Olivas and Barbosa-Cánovas (2008) |
| Kefiran | – | – | 2.7 | 40.9 | Piermaria et al. (2009) |
| PP | – | 47 | 933 | 798 | Gorna, Hund, Vučak, Gröhn, and Wegner (2008) |
| HDPE | – | 38 | 531 | 631 | Gorna et al. (2008) |

[a] After immersion in a $CaCl_2$ solution for 1 min.

**Table 2**
Water sorption coefficients, diffusion coefficients and water vapour permeability for the two driving forces studied.

| ΔRH (%) | $S_1$ ($\times 10^{-5}$ $g_{water}/g_{solids}$ Pa) | $S_2$ ($\times 10^{-5}$ $g_{water}/g_{solids}$ Pa) | $D_{eff}$ ($\times 10^{-12}$ $m^2/s$) | WVP ($\times 10^{-11}$ mol/m s Pa) |
|---|---|---|---|---|
| 92.0–64.8 | 14.9 | 7.8 | 2.3 ± 0.1 | 5.4 ± 0.8 |
| 64.8–22.0 | 5.7 | 2.5 | 2.8 ± 0.2 | 1.1 ± 0.2 |

(4.5–9.5 × $10^{-11}$ mol m/$m^2$ s Pa; Alves et al., 2010), in which the same procedure was used to estimate the effect of mass transfer resistance of the stagnant air below the test film.

### 3.9. $CO_2$ permeability

Before the permeability measurements, the film samples were equilibrated at controlled temperature and relative humidity, which eventually led to a water content of 7 ± 2% (dry basis) in the polymeric matrix. The determined permeability to carbon dioxide was (0.20 ± 0.03) × $10^{-15}$ mol m/$m^2$ s Pa. This value is quite low, and inferior to those referred for some synthetic polymers, such as LPDE, 4.2 × $10^{-15}$ mol m/$m^2$ s Pa (Gontard, Thibault, Cuq, & Guilbert, 1996), and PP, 0.9 × $10^{-15}$ mol m/$m^2$ s Pa (Costamagna, Strumia, López-González, & Riande, 2007). Since gas permeability of hydrophilic films is extremely dependent on their hydration degree, as presented by Gontard et al. (1996) for wheat gluten films, it becomes difficult to compare barrier properties presented by different authors, since it must be carried out for the same water content. Nevertheless, we may say that the value determined for the EPS film is two orders of magnitude higher than that presented for chitosan films at RH = 0% (0.0018 × $10^{-15}$ mol m/$m^2$ s Pa; Gontard et al., 1996), and much lower than that measured for methylcellulose/poly(ethylene glycol) films, also at RH = 0% (29.9 × $10^{-15}$ mol m/$m^2$ s Pa; Gontard et al., 1996).

### 3.10. Biological degradation

Samples of EPS films, as well as of LDPE and κ-carrageenan films (Fig. 6(a)–(c), respectively), were placed in agar plates, containing a nutrient-rich medium. An intense microbial growth was observed, which covered the EPS film sample surface within 8 days. The assay was extended up to 28 days (Fig. 6(d)), when complete film disintegration was confirmed, with some remnants totally mixed with the agar gel. Although a similar behaviour was detected with κ-carrageenan (Fig. 6(e)), microbial growth on the film surface was somewhat less intense and the films still maintained some mechanical strength. In contrast with the EPS film sample, it was possible to recover κ-carrageenan film from the plate. However, upon washing with water, the κ-carrageenan film was fragmented. Regarding the LDPE sample, as expected, there was no degradation, being recovered intact after the 28-day assay (Fig. 6(f)). From the results obtained, we may expect the EPS film to be easily degraded by the action of soil microorganisms.

## 4. Conclusions

Biodegradable films for food packaging were developed using a novel galactose-rich microbial polysaccharide. This value-added biomaterial was produced by an innovative process, based on the application of glycerol rich byproduct from the biodiesel industry as the sole carbon source. The films were prepared by casting an aqueous solution from purified biopolymer, followed by drying at controlled temperature. They were quite transparent with a good physical integrity when handled, even though showing some stiffness, with a low strain at break and a high Young modulus, when subjected to tensile tests.

The polymer revealed the capacity to form autocrosslinking reactions upon drying, under acidic conditions, resulting on films with a very low solubility in water and a significant swelling behaviour. The films presented an high water vapour permeability, but exhibited good barrier properties to carbon dioxide, better than some synthetic polymers (e.g. LDPE and PP).

Preliminary tests regarding the films biodegradability revealed a good biodegradation in a 28-day experiment in agar plates with an inocullum prepared from a soil sample.

The results obtained are rather promising regarding the ability of the novel microbial polysaccharide to produce biodegradable films, as they were obtained only with the biopolymer itself. The aqueous formulation may be further designed to form films for specific applications, with the use of additives (e.g. plasticizers, emulsifiers, nanocomposites). Furthermore, there is a huge potential to incorporate the polysaccharide films in multilayered structures, in which they would imprint very good gas barrier properties.

## Acknowledgements

The authors acknowledge Fábrica Torrejana de Biocombustíveis SA, Portugal, for supplying the glycerol byproduct from the biodiesel production, and Prof. Maria João Melo from REQUIMTE/CQFB – Departamento de Química, FCT/UNL for helping with FTIR analysis. The work was financially supported by 73100 Lda, under the project "Production of biopolymers from glycerol".

## References

Aider, M. (2010). Chitosan application for active bio-based films production and potential in the food industry: Review. *LWT - Food Science and Technology*, *43*, 837–842.
Alves, V. D., Costa, N., & Coelhoso, I. M. (2010). Barrier properties of biodegradable composite films based on kappa-carrageenan/pectin blends and mica flakes. *Carbohydrate Polymers*, *79*, 269–276.
Alves, V. D., Hilliou, L., Larotonda, F. D. S., Coelhoso, I. M., Gonçalves, M. P., & Sereno, A. M. (personal communication). Characterization of model edible films using hydrocolloids and pectins. In *9th international chemical engineering conference (Chempor 2005)*.
Bertuzzi, M. A., Vidaurre, E. F. C., Armada, M., & Gottifredi, J. C. (2007). Water vapor permeability of edible starch based films. *Journal of Food Engineering*, *80*, 972–978.
Collins, M. N., & Birkinshaw, C. (2008). Physical properties of crosslinked hyaluronic acid hydrogels. *Journal of Material Science: Materials in Medicine*, *19*, 3335–3343.
Costamagna, V., Strumia, M., López-González, M., & Riande, E. (2007). Gas transport in surface grafted polypropylene films with poly(acrylic acid) chains. *Journal of Polymer Science Part B: Polymer Physics*, *45*(17), 2421–2431.
da Silva, M. A., Bierhalz, A. C. K., & Kieckbusch, T. G. (2009). Alginate and pectin composite films crosslinked with $Ca^{2+}$ ions: Effect of the plasticizer concentration. *Carbohydrate Polymers*, *77*, 736–742.
de Moura, M. R., Aouada, F. A., Avena-Bustillos, R. J., McHugh, T. H., Krochta, J. M., & Mattoso, L. H. C. (2009). Improved barrier and mechanical properties of novel hydroxypropyl methylcellulose edible films with chitosan/tripolyphosphate nanoparticles. *Journal of Food Engineering*, *92*, 448–453.
Fabra, M. J., Talens, P., & Chiralt, A. (2008). Effect of alginate and λ-carrageenan on tensile properties and water vapour permeability of sodium caseinate-lipid based films. *Carbohydrate Polymers*, *74*, 419–426.
Freitas, F., Alves, V. D., Carvalheira, M., Costa, N., Oliveira, R., & Reis, M. A. M. (2009). Emulsifying behaviour and rheological properties of the extracellular polysaccharide produced by *Pseudomonas oleovorans* grown on glycerol byproduct. *Carbohydrate Polymers*, *78*, 549–556.
Freitas, F., Alves, V. D., Pais, J., Costa, N., Oliveira, C., Mafra, L., et al. (2009). Characterization of an extracellular polysaccharide produced by a *Pseudomonas* strain grown on glycerol. *Bioresource Technolology*, *100*, 859–865.
García-Ochoa, F., Santos, V. E., Casas, J. A., & Gómez, E. (2000). Xanthan gum: Production, recovery, and properties. *Biotechnology Advances*, *18*, 549–579.
Gennadios, A., Weller, C. L., & Gooding, C. H. (1994). Measurement errors in water vapor permeability of highly permeable, hydrophilic edible films. *Journal of Food Engineering*, *21*, 395–409.

Gontard, N, Thibault, R., Cuq, B., & Guilbert, S. (1996). Influence of relative humidity and film composition on oxygen and carbon dioxide permeabilities of edible films. *Journal Agricultural and Food Chemistry*, *44*, 1064–1069.

Gorna, K., Hund, M., Vučak, M., Gröhn, F., & Wegner, G. (2008). Amorphous calcium carbonate in form of spherical nanosized particles and its application as fillers for polymers. *Materials Science and Engineering A*, *477*, 217–225.

Greenspan, L. (1977). Humidity fixed points of binary saturated aqueous solutions. *Journal of Research of NBSA - Physics and Chemistry*, *81*. A(1)-89.

Hilliou, L., Freitas, F., Oliveira, R., Reis, M. A. M., Lespineux, D., Grandfils, C., et al. (2009). Solution properties of an exopolysaccharide from a *Pseudomonas* strain obtained using glycerol as sole carbon source. *Carbohydrate Polymers*, *78*, 526–532.

Hilliou, L., Larotonda, F. D. S., Abreu, P., Ramos, A. M., Sereno, A. M., & Gonçalves, M. P. (2006). Effect of extraction parameters on the chemical structure and gel properties of κ/ι-hybrid carrageenans obtained from *Mastocarpus stellatus*. *Biomolecular Engineering*, *23*(4), 201–208.

Labuza, T. P., Kaanane, A., & Chen, J. Y. (1985). Effect of temperature on the moisture sorption isotherms and water activity shift of two dehydrated foods. *Journal of Food Science*, *50*, 385–391.

Lafargue, D., Lourdin, D., & Doublier, J. L. (2007). Film-forming properties of a modified starch/κ-carrageenan mixture in relation to its rheological behaviour. *Carbohydrate Polymers*, *70*, 101–111.

Larotonda, F. D. S., Matsui, K. N., Sobral, P. J. A., & Laurindo, J. B. (2005). Hygroscopicity and water vapor permeability of Kraft paper impregnated with starch acetate. *Journal of Food Engineering*, *71*, 394–402.

Lazaridou, A., & Biliaderis, C. G. (2002). Thermophysical properties of chitosan, chitosan–starch and chitosan–pullulan films near the glass transition. *Carbohydrate Polymers*, *48*, 179–190.

Mali, S., Grossmann, M. V. E., García, M. A., Martino, M. N., & Zaritzky, N. E. (2006). Effects of controlled storage on thermal, mechanical and barrier properties of plasticized films from different starch sources. *Journal of Food Engineering*, *75*, 453–460.

Müller, C. M. O, Laurindo, J. B., & Yamashita, F. (2009). Effect of cellulose fibers on the crystallinity and mechanical properties of starch-based films at different relative humidity values. *Carbohydrate Polymers*, *77*, 293–299.

Nisperos-Carriedo, M. (1994). Edible coatings and films based on polysaccharides. In J. M. Krochta, E. A. Baldwin, & M. Nisperos-Carriedo (Eds.), *Edible coatings and films to improve food quality* (pp. 305–335). Lancaster: Technomic Publishing Company Inc.

Okamoto, A., & Miyoshi, T. (2002). In J. Kennedy, G. Phillips, & P. Williams (Eds.), *A biocompatible gel of hyaluronan*. Hyaluronan, Cambridge: Woodhead Publishing Limited.

Olivas, G. I., & Barbosa-Cánovas, G. V. (2008). Alginate–calcium films: Water vapor permeability and mechanical properties as affected by plasticizer and relative humidity. *LWT*, *41*, 359–366.

Piermaria, J. A., Pinotti, A., García, M. A., & Abraham, A. G. (2009). Films based on kefiran, an exopolysaccharide obtained from kefir grain: Development and characterization. *Food Hydrocolloids*, *23*, 684–690.

Singh, R. S., Saini, G. K., & Kennedy, J. F. (2008). Pullulan: Microbial sources, production and applications. *Carbohydrate Polymers*, *73*, 515–531.

Siracusa, V., Rocculi, P., Romani, S., & Dalla Rosa, M. (2008). Biodegradable polymers for food packaging: A review. *Trends in Food Science & Technology*, *19*, 634–643.

Soares, R. M. D., Lima, A. M. F., Oliveira, R. V. B., Pires, A. T. N., & Soldi, V. (2005). Thermal degradation of biodegradable edible films based on xanthan and starches from different sources. *Polymer Degradation and Stability*, *90*, 449–454.

Sun, F., & Zhitomirsky, I. (2009). Electrodeposition of hyaluronic acid and composite films. *Surface Engineering*, *25*, 621–627.

Synytsya, A., Copikova, J., Matejka, P., & Machovic, V. (2003). Fourier transform Raman and infrared spectroscopy of pectins. *Carbohydrate Polymers*, *54*, 97–106.

Xu, X., Li, B., Kennedy, J. F., Xie, B. J., & Huang, M. (2007). Characterization of konjac glucomannan–gellan gum blend films and their suitability for release of nisin incorporated therein. *Carbohydrate Polymers*, *70*, 192–197.